Experimental Study and Thermodynamic Assessment of the Ni-Mo-Ta Ternary System

YUWEN CUI, XIAOGANG LU, and ZHANPENG JIN

Phase equilibrium data of the Ni-Mo-Ta system at 1473, 1373, and 1173 K were determined by means of diffusion triple and electron probe microanalysis (EPMA) techniques in this article. From the present experimental results and literature data, the Ni-Mo-Ta system was thermodynamically assessed using the CALPHAD method. A set of consistent thermodynamic parameters of each phase was obtained. A number of calculated isothermal sections are presented and compared with experimental data. They are in reasonable agreement. The present calculation was successfully used to analyze the solidification behavior of two alloys. Two subsystems, Ni-Mo and Mo-Ta, were assessed prior to the assessment of the ternary system.

I. INTRODUCTION

THE Ni-Mo-Ta ternary system is of great interest in relation to the development of some Ni-based superalloys. This system has been studied by several investigators. The first investigation of the Ni-Mo-Ta system was carried out by Virkar and Raman.[1] An isothermal section at 1173 K was determined; nevertheless, because the single-phase boundaries were not determined and the number of alloys was too few to determine all three phase boundaries accurately, their results were considered to be rather tentative. By means of electron probe microanalysis (EPMA) and X-ray diffraction, Chakravorty and West[2] determined two partial isothermal sections at 1523 and 1273 K. Some data for 1173 K were also obtained. In addition, they suggested a partial liquidus projection diagram based on the analysis of as-cast alloys. The most notable discrepancy between those two groups is that Virkar and Raman found that Ni_3Ta and Ni_3Mo can form continuous series of solid solution at 1173 K, while Chakravorty and West stated that they cannot. Gupta[3] critically evaluated the previous works of the Ni-Mo-Ta system. Furthermore, he proposed another probable liquidus projection.

Kaufman[4] published a tentative calculation of the Ni-Mo-Ta ternary system based on the limited experimental information, in which no ternary solution and compound parameters were employed. Accordingly, it is the objective of this work to determine the phase equilibrium data of the Ni-Mo-Ta system in more detail and to develop a set of consistent thermodynamic descriptions of this system using the CALPHAD method.

II. EXPERIMENT

The diffusion couple technique, as an effective and powerful approach to determine phase diagrams, plays a dominant role in the study of complex metallic systems. This method was thus adopted in our work.

Starting materials were electrolytic nickel (99.97 pct), pure molybdenum bar (99.97 pct), and pure tantalum bar (99.95 pct), provided by GE Company (Schenectady, NY).

At first, the Mo-Ta binary couple was prepared by diffusion welding in a GLEEBLE-1500-type Thermal Simulator. The welding was conducted in vacuum (better than 3×10^{-3} Pa) at 1473 to 1573 K under a certain force for 20 to 30 minutes.

The binary couples and Ni pieces were then polished and welded together, also in the GLEEBLE-1500-type Thermal Simulator, to form well-contacted Ni-Mo-Ta diffusion triples. Figure 1 illustrates the construction of the Ni-Mo-Ta diffusion triple. The triples were sealed in evacuated silica capsules with a vacuum (3×10^{-3} Pa) and heated in a GK-2B-type diffusion furnace at 1473 K for 200 hours, at 1373 K for 500 hours, and at 1173 K for 1000 hours. The temperature was controlled within ± 5 K. After annealing, the triples were air quenched. The air-quenched triples were polished parallel to the diffusion direction.

The microstructure was observed by optical microscopy, and the local composition was analyzed by EPMA performed on CAMEBAX SX-50.

Figures 2(a) and (b) show the backscattered electron images of the Ni-Mo-Ta diffusion triples annealed at 1473 and 1373 K, and Figures 2(d) and (e) present their schematic diagrams of phase distribution. From the EPMA analysis, six intermediate phases, Ni_8Ta, Ni_3Ta, Ni_2Ta, NiTa, $NiTa_2$, and NiMo, were formed at both temperatures. Figures 2(c) and (f) show the backscattered electron image and the schematic diagram of phase distribution of the Ni-Mo-Ta diffusion triple annealed at 1173 K for 1000 hours. As can be seen from these two figures, two intermediate phases, Ni_3Ta and NiMo, were evidently detected as well as very thin diffusion layers of Ni_2Ta and NiTa. The absence of other equilibrium phases is probably a result of their very slow growth rates at this temperature or the definitive resolution of CAMEBAX SX-50.

All the determined equilibrium data are listed in Tables I through III. The listed tie-lines were obtained by extrapolation of the concentration profile across the boundary between pairs of phases. The tie triangles were measured by locating the three-phase equilibria, and the listed ones are the average

YUWEN CUI, Postdoctoral Candidate, and ZHANPENG JIN, Professor, are with the Department of Materials Science and Engineering, Central South University of Technology, Hunan 410083, People's Republic of China. XIAOGANG LU, Postdoctoral Candidate, on leave from the Department of Materials Science and Engineering, Central South University of Technology, is with the Department of Materials Science and Engineering, Royal Institute of Technology, S-10044 Stockholm, Sweden.

Manuscript submitted August 24, 1998.

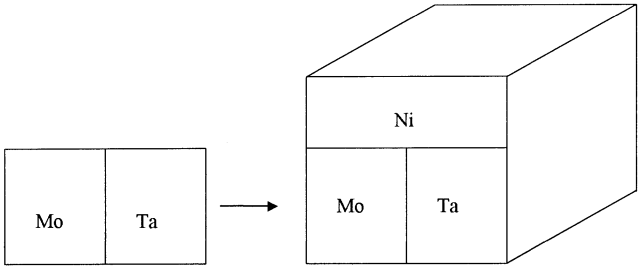

Fig. 1—The schematic diagram of the construction of the Ni-Mo-Ta diffusion triple.

values of several individual measurements. Nevertheless, because some EPMA data appear to be somewhat scattering and anomalous in their respective concentration profiles, reasonable and appropriate extrapolations were impossible; thus, only indicative equilibrium data can be estimated. Those data were considered to be tentative and have great uncertainty; thus, they were not utilized in the present assessment, as indicated in Tables I through III in the column entitled "Data Used." In addition, the data involving the Ni_8Ta phase at 1473 and 1373 K were not given. The reason is that the compositions of fcc and Ni_8Ta are too close to distinguish clearly in the backscattered images. Therefore, it is not possible to get a reliable extrapolation from their concentration profiles. The data for Ni_8Ta at 1173 K were also unavailable because they were absent from the diffusion triple.

Comparing the present data at 1173 K and those from Chakravorty and West,[2] the (fcc + Ni_3Ta) two-phase region obtained in this work almost reaches the vicinity of the Ni-Mo system. In fact, this two-phase region together with the Ni_3Ta single-phase region already wholly overlaps with the

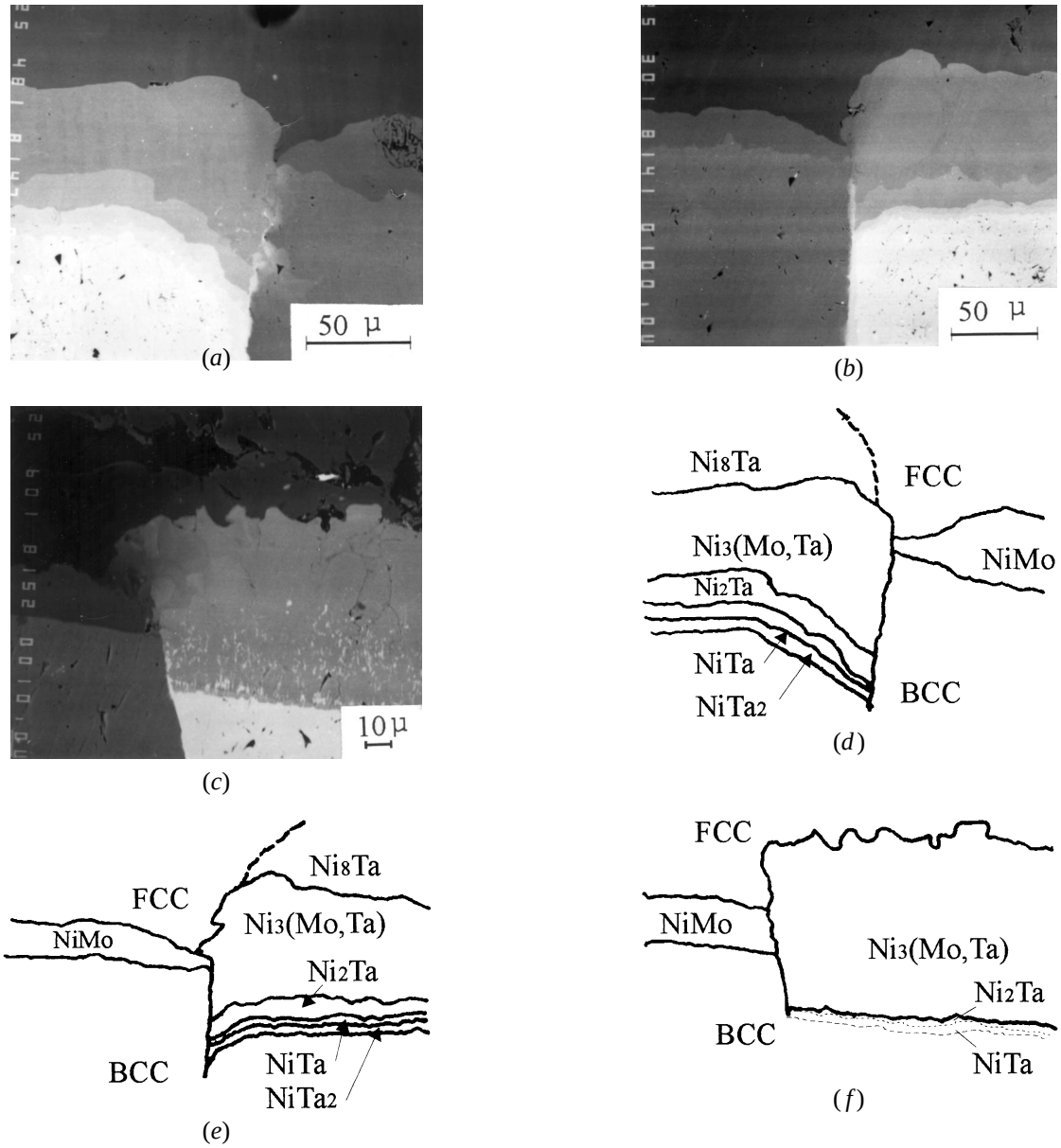

Fig. 2—(*a*) through (*c*) The backscattered electron images of the Ni-Mo-Ta diffusion triple. (*d*) through (*f*) The schematic diagrams of phase distribution. Annealing times were (*a*) and (*d*) 1473 K for 200 h, (*b*) and (*e*) 1373 K for 500 h, and (*c*) and (*f*) 1173 K for 1000 h.

Table I. The Equilibrium Data Determined by EPMA in the Ni-Mo-Ta Diffusion Triple at 1473 K (Atomic Percent)

$Ni_3(Mo, Ta)$		NiMo		Data	$Ni_3(Mo, Ta)$		Bcc		Data
Mo	Ta	Mo	Ta	Used	Mo	Ta	Mo	Ta	Used
12.1	12.7	45.5	2.4	yes	1.5	24.6	74.7	20.5	no
11.0	13.3	46.6	2.0	yes	—	—	75.0	22.5	no
12.0	13.1	47.1	2.2	yes	2.2	22.7	87.8	10.2	yes
NiMo		Fcc			$Ni_3(Mo, Ta)$		Fcc		
Mo	Ta	Mo	Ta		Mo	Ta	Mo	Ta	
46.6	1.7	19.6	4.1	yes	0.1	23.4	0.8	12.2	no
48.5	1.6	20.1	4.2	yes	11.0	13.7	18.0	5.0	yes
48.3	0.7	18.0	8.0	no	11.5	13.5	19.0	4.6	no
NiMo		Bcc			12.0	12.4	19.6	4.2	yes
Mo	Ta	Mo	Ta		12.7	12.0	18.8	4.3	yes
47.7	2.5	93.9	4.0	yes	10.4	13.3	12.9	6.0	yes
NiTa		Bcc			0.1	22.2	3.3	10.4	yes
Mo	Ta	Mo	Ta		2.1	21.3	5.3	9.4	yes
1.8	54.0	37.8	60.2	no	5.0	18.3	8.0	8,.0	yes
3.5	49.9	49.8	49.1	yes	9.4	14.6	10.1	6.8	yes
Ni_2Ta		$Ni_3(Mo, Ta)$			NiTa		Ni_2Ta		
Mo	Ta	Mo	Ta		Mo	Ta	Mo	Ta	
0.1	34.2	0.1	25.7	yes	5.7	47.1	0.3	34.9	yes

NiMo		$Ni_3(Mo, Ta)$		Fcc			Ni_2Ta		$Ni_3(Mo, Ta)$		Bcc		
Mo	Ta	Mo	Ta	Mo	Ta		Mo	Ta	Mo	Ta	Mo	Ta	
45.7	1.9	15.4	11.2	19.6	4.1	yes	0.1	33.4	3.0	26.1	55.8	41.4	no

Table II. The Equilibrium Data Determined by EPMA in the Ni-Mo-Ta Diffusion Triple at 1373 K (Atomic Percent)

$Ni_3(Mo, Ta)$		NiMo		Data	$Ni_3(Mo, Ta)$		Bcc		Data
Mo	Ta	Mo	Ta	Used	Mo	Ta	Mo	Ta	Used
16.2	8.4	48.5	0.6	yes	1.9	22.9	91.8	5.4	yes
16.0	9.1	49.4	0.4	yes	17.2	7.6	—	—	no
16.4	9.2	50.0	0.7	yes	—	—	—	—	—
fcc		NiMo			$Ni_3(Mo, Ta)$		Fcc		
Mo	Ta	Mo	Ta		Mo	Ta	Mo	Ta	
20.8	0.2	48.4	0.4	yes	16.0	8.9	19.5	2.7	yes
21.0	2.5	48.8	0.5	yes	15.9	8.7	20.0	2.7	yes
20.5	2.7	49.0	0.6	yes	17.0	7.8	20.5	2.5	yes
21.8	2.3	48.8	0.5	yes	12.4	11.2	13.0	4.7	yes
					4.5	19.0	5.0	8.1	yes
					6.5	16.9	6.6	7.9	yes
					13.0	9.7	14.0	4.1	yes
					8.8	14.0	10.9	5.2	yes
$NiTa_2$		Bcc							
Mo	Ta	Mo	Ta						
0.2	66.2	0.4	98.5	yes					
Ni_2Ta		$Ni_3(Mo, Ta)$			NiTa		Ni_2Ta		
Mo	Ta	Mo	Ta		Mo	Ta	Mo	Ta	
0.1	33.0	0.1	24.9	yes	0.1	50.4	0.1	32.6	yes

NiMo		$Ni_3(Mo, Ta)$		Bcc			Ni_2Ta		$Ni_3(Mo, Ta)$		Bcc		
Mo	Ta	Mo	Ta	Mo	Ta		Mo	Ta	Mo	Ta	Mo	Ta	
		12.4	12.8			no	0.3	33.4	0.7	25.8	61.7	24.7	yes

Table III. The Equilibrium Data Determined by EPMA in the Ni-Mo-Ta Diffusion Triple at 1173 K (Atomic Percent)

Ni_3(MO, Ta)		NiMo		Data	Ni_3(Mo, Ta)		Fcc		Data
Mo	Ta	Mo	Ta	Used	Mo	Ta	Mo	Ta	Used
10.6	14.3	48.9	1.7	yes	0.0	24.6	0.3	11.5	no
15.3	9.3	50.8	0.0	yes	13.2	9.9	10.8	4.1	yes
Ni_3(Mo, Ta)		Ni_2Ta			14.3	9.2	12.5	3.0	yes
Mo	Ta	Mo	Ta		7.5	15.5	5.7	6.8	yes
1.0	25.9	0.7	32.2	yes	9.6	13.3	6.5	6.0	yes
Ni_2Ta		NiTa			16.5	7.5	14.2	2.0	yes
Mo	Ta	Mo	Ta		19.3	4.5	15.7	1.4	yes
0.0	33.7	0.6	52.2	no					

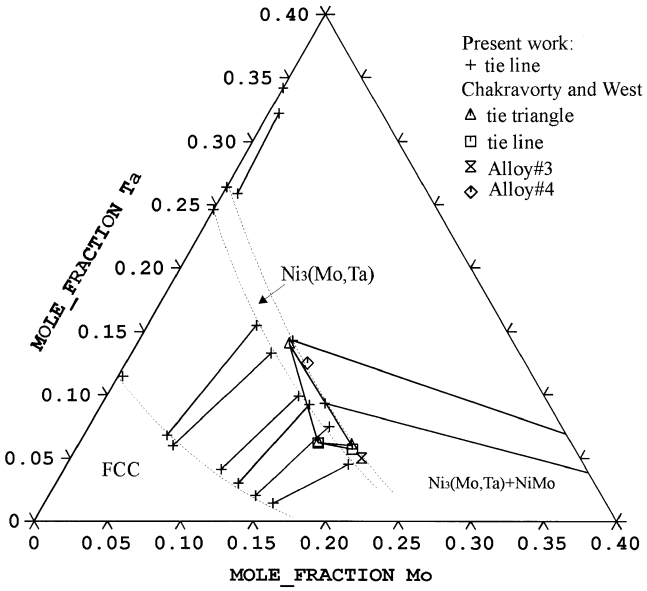

Fig. 3—Comparison between the present experimental data at 1173 K and those obtained by Chakravorty and West.[2]

(Ni_3Mo + fcc + Ni_3Ta) three-phase region revealed by Chakravorty and West, as presented in Figure 3. In the study of Chakravorty and West, neither tie-line nor tie-triangle, which was used to verify that Ni_3Ta and Ni_3Mo cannot form complete solid solution, passed through their respective nominal alloy compositions. It is therefore reasonable to consider that those data are not reliable enough. In addition, Ni_3Mo (isotypic with Cu_3Ti) and Ni_3Ta (isotypic with Cu_3Ti or Pt_3Ta) have similar crystal structure, very similar lattice parameters, and a small difference between the CN12 atomic radii of Mo and Ta (r_{Ta} is only 5 pct larger than r_{Mo}).[3] From these findings, along with the study of Virkar and Raman,[1] Ni_3Ta phase and Ni_3Mo should be treated as one phase in the Ni-Mo-Ta ternary system. In this work, it was designated as Ni_3(Mo, Ta).

III. THERMODYNAMIC ASSESSMENT

A Binary Boundary Systems

1. *Ni-Ta system*

The Ni-Ta system was previously assessed by Kaufman[5] and Ansara and Selleby.[6] Recently, Cui and Jin[7] reassessed this system based upon new experimental data. The thermodynamic assessment by Cui and Jin was adopted in this work. The calculated Ni-Ta phase diagram is reproduced in Figure 4.

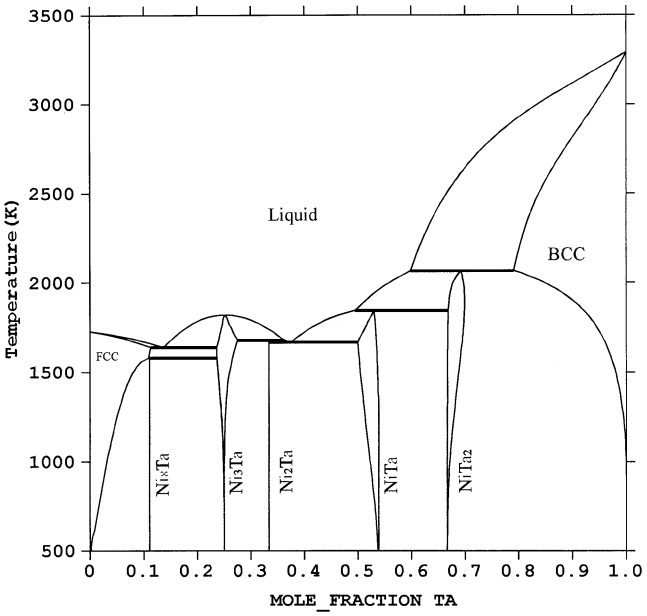

Fig. 4—The calculated Ni-Ta system by Cui and Jin.[7]

2. *Ni-Mo system*

The Ni-Mo system was investigated by Frisk.[8] In her assessment, the Ni_3Mo phase was treated as stoichiometric compound. However, Ni_3Ta, which has a similar crystal structure to Ni_3Mo, was described by a two-sublattice model $(Ni, Ta)_3(Ni, Ta)_1$ in the Ni-Ta system.[7] Due to the fact that Ni_3Ta and Ni_3Mo were treated as one phase Ni_3(Mo, Ta) in the Ni-Mo-Ta ternary system, it is necessary to remodel the Ni_3Mo phase as $(Ni, Mo)_3 (Ni, Mo)_1$ so that it has a consistent model with Ni_3Ta for the calculation of ternary or higher order system. In addition, Ni_4Mo is assumed to decompose into fcc(Ni) and Ni_3Mo at about 317 K in the assessment by Frisk, which is unreasonable without any direct experimental information. Accordingly, the Ni-Mo system was modified in the present article.

A detailed review of experimental data and descriptions of the thermodynamic model were already given in the assessment by Frisk.[8] It is thus unnecessary to repeat them in the present article. Similar to the model of Ni_3Ta, the Ni_3Mo phase was modeled by a two-sublattice model $(Ni, Mo)_3(Ni, Mo)_1$.

The assessed parameters of each phase in the present work are summarized in Table IV. The modified Ni-Mo phase diagram is presented in Figure 5. Figure 6 shows the calculated Ni-rich portion of the Ni-Mo system together with experimental data.[9,10] Besides the two improvements on the aforementioned problems, the fcc(Ni)/fcc(Ni) + NiMo phase boundary was moved to higher Mo contents to make a compromise between the experimental points by Casselton and Hume-Rothery[9] and those by Heijwegen and Rieck.[10]

The calculated and measured values of the enthalpy of formation[11,12] of the NiMo phase are in good agreement, as presented in Figure 7.

Table IV. The Assessed Parameters of Ni-Mo, Mo-Ta, and Ni-Mo-Ta Systems in the Present Work*

Liquid phase (description: Redlich–Kister)
$^{0}L^{liq}_{Ni,Mo} = -40{,}224 + 15.75 * T$
$^{1}L^{liq}_{Ni,Mo} = 3347$
$^{0}L^{liq}_{Mo,Ta} = -73{,}477$
$^{1}L^{liq}_{Mo,Ta} = -4091$
$L^{liq}_{Ni,Mo,Ta} = 30{,}000$
Bcc phase (description: Redlich–Kister)
$^{0}L^{bcc}_{Ni,Mo} = 42{,}679$
$^{1}L^{bcc}_{Ni,Mo} = 4825$
$^{0}L^{bcc}_{Mo,Ta} = -69{,}360$
$^{1}L^{bcc}_{Mo,Ta} = -4190$
$L^{bcc}_{Ni,Mo,Ta} = -61{,}977$
Fcc phase (description: Redlich–Kister)
$^{0}L^{fcc}_{Ni,Mo} = -3765$
$^{1}L^{fcc}_{Ni,Mo} = 12{,}548$
$^{0}L^{fcc}_{Mo,Ta} = -6572$
$L^{fcc}_{Ni,Mo,Ta} = -5800$
Ni_8 Ta phase (description: $(Ni)_8$ (Mo, Ta)$_1$)
$^{\circ}G^{Ni8Ta}_{Ni:Mo} = 8 * {}^{\circ}G^{fcc}_{Ni} + {}^{\circ}G^{bcc}_{Mo} + 8 * (-2300)$
Ni_3(Mo, Ta) phase (description: (Ni, Mo, Ta)$_3$(Ni, Mo, Ta)$_1$)
$^{\circ}G^{Ni3(Mo,Ta)}_{Mo:Mo} = 180{,}000 + 4 * {}^{\circ}G^{bcc}_{Mo}$
$^{\circ}G^{Ni3(Mo,Ta)}_{Ni:Mo} = 4 * (-3363 - 0.02 * T) + {}^{\circ}G^{bcc}_{Mo} + 3 * {}^{\circ}G^{fcc}_{Ni}$
$^{\circ}G^{Ni3(Mo,Ta)}_{Ta:Mo} = 80{,}000 + 3 * {}^{\circ}G^{bcc}_{Ta} + {}^{\circ}G^{bcc}_{Mo}$
$^{\circ}G^{Ni3(Mo,Ta)}_{Mo:Ni} = 4 * (53{,}363 + 0.02 * T) + 3 * {}^{\circ}G^{bcc}_{Mo} + {}^{\circ}G^{fcc}_{Ni}$
$^{\circ}G^{Ni3(Mo,Ta)}_{Mo:Ta} = 100{,}000 + {}^{\circ}G^{bcc}_{Ta} + 3 * {}^{\circ}G^{bcc}_{Mo}$
$^{\circ}G^{Ni3(Mo,Ta)}_{Ni,\,Mo:Ni} = {}^{\circ}G^{Ni3(Mo,Ta)}_{Ni,Mo:Mo} = {}^{\circ}G^{Ni3(Mo,Ta)}_{Ni,Mo:Ta} = -4080$
$^{\circ}G^{Ni3(Mo,Ta)}_{Ni:Ni,Mo} = {}^{\circ}G^{Ni3(Mo,Ta)}_{Mo:Ni,Mo} = {}^{\circ}G^{Ni3(Mo,Ta)}_{Ta:Ni,Mo} = -3804$
NiTa phase (description: (Ni, Ta)$_1$(Mo, Ta)$_4$(Ni, Ta)$_2$(Ni)$_6$)
$^{\circ}G^{NiTa}_{Ni:Mo:Ni:Ni} = 7 * {}^{\circ}G^{fcc}_{Ni} + 2 * {}^{\circ}G^{bcc}_{Ni} + 4 * {}^{\circ}G^{bcc}_{Mo}$
$^{\circ}G^{NiTa}_{Ta:Mo:Ni:Ni} = {}^{\circ}G^{fcc}_{Ta} + 4 * {}^{\circ}G^{bcc}_{Mo} + 2 * {}^{\circ}G^{bcc}_{Ni} + 6 * {}^{\circ}G^{fcc}_{Ni}$
$^{\circ}G^{NiTa}_{Ni:Mo:Ta:Ni} = -181{,}922 + 7 * {}^{\circ}G^{fcc}_{Ni} + 4 * {}^{\circ}G^{bcc}_{Mo} + 2 * {}^{\circ}G^{bcc}_{Ta}$
$^{\circ}G^{NiTa}_{Ta:Mo:Ta:Ni} = -276{,}900 + {}^{\circ}G^{fcc}_{Ta} + 4 * {}^{\circ}G^{bcc}_{Mo} + 2 * {}^{\circ}G^{bcc}_{Ta} + 6 * {}^{\circ}G^{fcc}_{Ni}$
$NiTa_2$ phase (description: (Ni, Mo, Ta)$_1$(Mo, Ta)$_2$)
$^{\circ}G^{NiTa2}_{Mo:Mo} = 40{,}000 + {}^{\circ}G^{bcc}_{Mo}$
$^{\circ}G^{NiTa2}_{Ni:Mo} = -1500 + 2 * {}^{\circ}G^{bcc}_{Mo} + {}^{\circ}G^{fcc}_{Ni}$
$^{\circ}G^{NiTa2}_{Ta:Mo} = 2 * {}^{\circ}G^{bcc}_{Mo} + {}^{\circ}G^{bcc}_{Ta}$
$^{\circ}G^{NiTa2}_{Mo:Ta} = {}^{\circ}G^{bcc}_{Mo} + 2 * {}^{\circ}G^{bcc}_{Ta}$
$^{\circ}G^{NiTa2}_{Ni,Mo:Mo} = {}^{\circ}G^{NiTa2}_{Ni,Mo:Ta} = -30{,}000$
$^{\circ}G^{NiTa2}_{Ni,Ta:Mo} = {}^{\circ}G^{NiTa2}_{Ni,Ta:Ta} = 15{,}840$
NiMo phase (description: $(Ni)_{24}$(Ni, Mo, Ta)$_{20}$(Mo, Ta)$_{12}$)
$^{\circ}G^{NiMo}_{Ni:Mo:Mo} = 56 * (-4687 + 26.336 * T - 3.408 * T * \ln(T)) + 24 * {}^{\circ}G^{fcc}_{Ni} + 32 * {}^{\circ}G^{bcc}_{Mo}$
$^{\circ}G^{NiMo}_{Ni:Ni:Mo} = 56 * (-1402.8 - 7.908 * T + 1.165 * T * \ln(T)) + 24 * {}^{\circ}G^{fcc}_{Ni} + 20 * {}^{\circ}G^{bcc}_{Ni} + 12 * {}^{\circ}G^{bcc}_{Mo}$
$^{\circ}G^{NiMo}_{Ni:Ta:Mo} = -1{,}224{,}888 + 12 * {}^{\circ}G^{bcc}_{Mo} + 24 * {}^{\circ}G^{fcc}_{Ni} + 20 * {}^{\circ}G^{bcc}_{Ta}$
$^{\circ}G^{NiMo}_{Ni:Mo:Ta} = -679{,}392 + 20 * {}^{\circ}G^{bcc}_{Mo} + 24 * {}^{\circ}G^{fcc}_{Ni} + 12 * {}^{\circ}G^{bcc}_{Ta}$
$^{\circ}G^{NiMo}_{Ni:Ni:Ta} = -1{,}203{,}776 + 44 * {}^{\circ}G^{fcc}_{Ni} + 12 * {}^{\circ}G^{bcc}_{Ta}$
$^{\circ}G^{NiMo}_{Ni:Ta:Ta} = 34{,}496 + 24 * {}^{\circ}G^{fcc}_{Ni} + 32 * {}^{\circ}G^{bcc}_{Ta}$

*Values for Liquid, Fcc, and Bcc are given in J/mol of atoms and in J/mol formula units for the intermediate phases.

3. *Mo-Ta system*

The Mo-Ta system was studied by Buckle,[13] Geach and Smith,[14] and Rudy.[15] They found that this binary system was an isomorphous system in which Mo and Ta form a continuous series of bcc solid solution. The currently accepted Mo-Ta system came from the compilation of Massalski *et al.*[16] Singhal and Worrel[17] determined the thermodynamic properties of solid Mo-Ta alloys between 1000 K and 1300 K using a galvanic cell. Their results show that the activities of Ta and Mo exhibit large negative deviation from ideality.

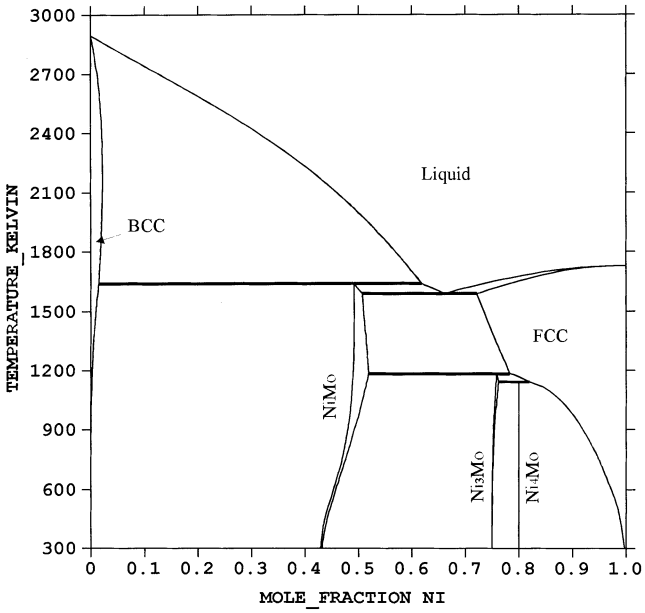

Fig. 5—The modified Ni-Mo system in present assessment.

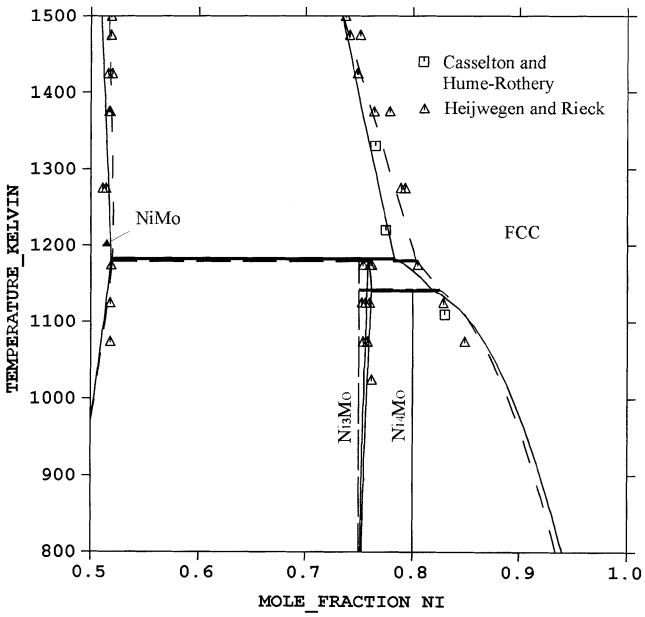

Fig. 6—The modified Ni-rich portion of the Ni-Mo system together with the experimental data. Dashed lines are the calculated results by Frisk.[8]

The equilibrium data evaluated in the compilation of Massalski *et al.*[16] were adopted in the present assessment. The data used in the assessment were read from the evaluated diagram at an interval of 5 at. pct Ta. The data of Singhal and Worrel[17] were accepted to assess the bcc phase. Their measured electromotive force values were transformed into the chemical potentials of Ta in bcc during the optimization.

In this work, both the liquid and bcc phases were treated as regular solution. The assessed parameters are listed in Table IV. The calculated Mo-Ta system is shown in Figure 8. The calculation shows good agreement with the evaluated data from Reference 16. Figure 9 presents the comparison between the calculated and the derived chemical potentials

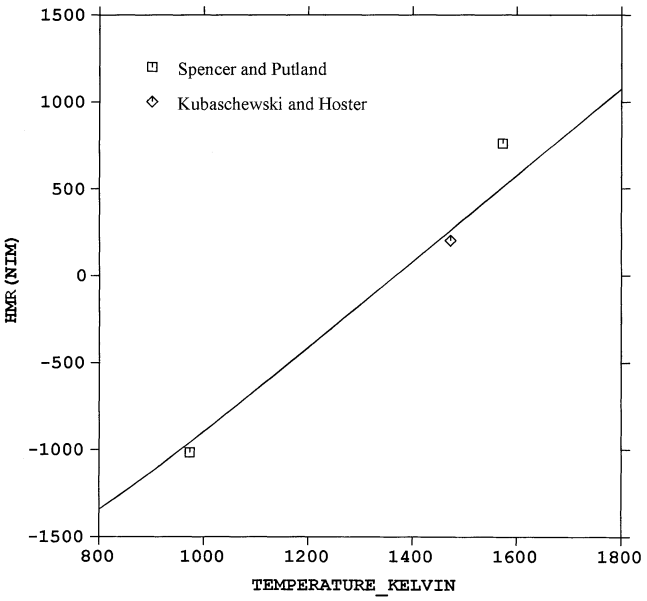

Fig. 7—Comparison between the calculated and measured values of the enthalpy of formation of the NiMo phase.

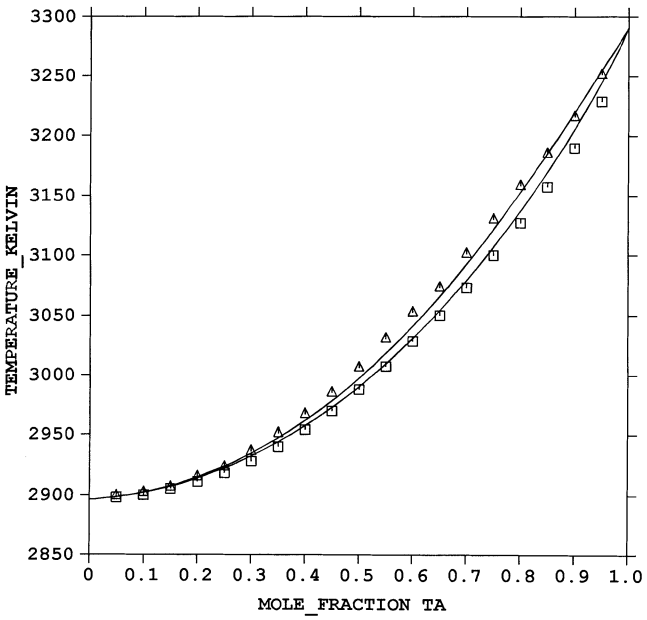

Fig. 8—The assessed Mo-Ta system together with the evaluated data.

of Ta in the bcc phase. It shows that, at Mo-rich portion, the calculated values are lower than the experimental points. However, the attempt to get a better fit was not made because it would result in an unacceptable reproduction of the experimental data involving the bcc phase in the calculation of the Ni-Mo-Ta ternary system.

B. *The Ternary System*

1. *Selection of the experimental data*

Because the isothermal section given by Virkar and Raman[1] was considered to be tentative, all their data were not adopted in the assessment. All the equilibrium data from Chakravorty and West[2] were employed in the assessment,

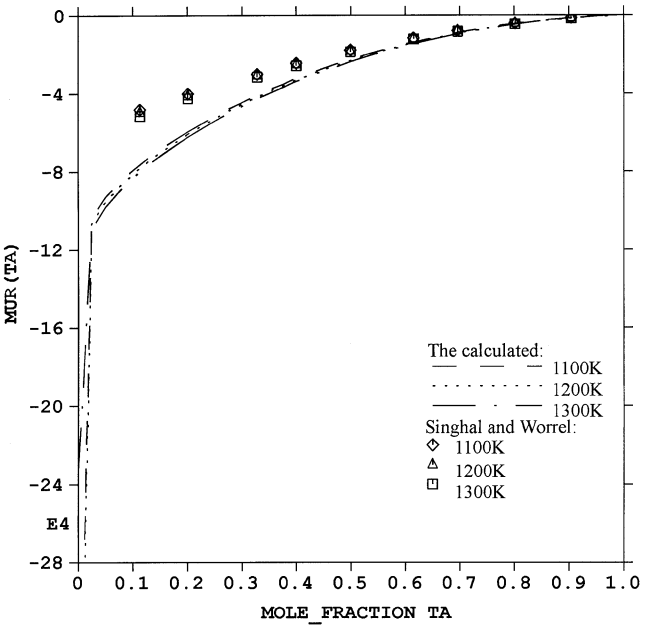

Fig. 9—Comparison between the calculated and derived chemical potentials of Ta in the bcc phase.

apart from those which may have great uncertainty. Those excluded data included the tie-lines that did not pass through the nominal alloy compositions.

Most data obtained from the present experiment were used in the assessment. However, as previously mentioned, some indicative data were not used. No thermochemical data are available.

2. *Thermodynamic model*

The substitutional solution model was used to describe bcc, fcc, and liquid. The model yields the following expression for the Gibbs energy:

$$G_m = x_{\mathrm{Ni}}\,{}^{\circ}G^{h}_{\mathrm{Ni}} + x_{\mathrm{Mo}}\,{}^{\circ}G^{h}_{\mathrm{Mo}} + x_{\mathrm{Ta}}\,{}^{\circ}G^{h}_{\mathrm{Ta}} + \mathrm{R}T(X_{\mathrm{Ni}} \ln X_{\mathrm{Ni}} + X_{\mathrm{Mo}} \ln X_{\mathrm{Mo}} + X_{\mathrm{Ta}} \ln X_{\mathrm{Ta}}) + {}^{e}G_m + G^{mo}_m \quad [1]$$

where ${}^{e}G_m$ is the excess Gibbs energy and can be expressed as follows:

$${}^{e}G_m = x_{\mathrm{Ni}}x_{\mathrm{Mo}}L_{\mathrm{Ni,Mo}} + x_{\mathrm{Ni}}x_{\mathrm{Ta}}L_{\mathrm{Ni,Ta}} + x_{\mathrm{Mo}}x_{\mathrm{Ta}}L_{\mathrm{Mo,Ta}} + x_{\mathrm{Ni}}x_{\mathrm{Mo}}x_{\mathrm{Ta}}L_{\mathrm{Ni,Mo,Ta}} \quad [2]$$

The parameter ${}^{\circ}G^{h}_{i}$ is the Gibbs energy of pure component i in a hypothetical nonmagnetic state and is taken from the database.[18] The term G^{mo}_m represents the contribution due to magnetic ordering. This term was assumed to be zero for the liquid phase. The three binary L parameters are taken from the corresponding binary systems.

For the description of the solubility of Mo in the binary stoichiometric phase Ni_8Ta, a formula $(Ni)_8(Mo, Ta)_1$ was yielded for Ni_8Ta, where Mo was assumed to substitute for Ta.

The experimental data of Chakravorty and West,[2] together with the present data, show that only negligible Mo can dissolve in the Ni_2Ta phase. Thereby, no ternary compound parameters were considered. For the Ni_4Mo phase, a similar treatment was taken into account.

As already mentioned, Ni_3Ta and Ni_3Mo were treated as one phase in the ternary system, which was denoted as $Ni_3(Mo, Ta)$. This treatment yields the model (Ni, Mo, Ta)$_3$(Ni, Mo, Ta)$_1$. The Gibbs energy for one mole of formula units can be expressed as follows:

$$\begin{aligned}G_m = {}& {}^1y_{Ni}({}^2y_{Ni}\,{}^\circ G_{Ni:Ni} + {}^2y_{Ta}\,{}^\circ G_{Ni:Ta} + {}^2y_{Mo}\,{}^\circ G_{Ni:Mo})\\ & + {}^1y_{Ta}({}^2y_{Ni}\,{}^\circ G_{Ta:Ni} + {}^2y_{Ta}\,{}^\circ G_{Ta:Ta} + {}^2y_{Mo}\,{}^\circ G_{Ta:Mo})\\ & + {}^1y_{Mo}({}^2y_{Ni}\,{}^\circ G_{Mo:Ni} + {}^2y_{Ta}\,{}^\circ G_{Mo:Ta} + {}^2y_{Mo}\,{}^\circ G_{Mo:Mo})\\ & + 3RT({}^1y_{Ni}\ln {}^1y_{Ni} + {}^1y_{Ta}\ln {}^1y_{Ta} + {}^1y_{Mo}\ln {}^1y_{Mo})\\ & + RT({}^2y_{Ni}\ln {}^2y_{Ni} + {}^2y_{Ta}\ln {}^2y_{Ta} + {}^2y_{Mo}\ln {}^2y_{Mo})\\ & + {}^1y_{Ni}\,{}^1y_{Ta}({}^2y_{Ni}L_{Ni,Ta:Ni} + {}^2y_{Ta}L_{Ni,Ta:Ta} + {}^2y_{Mo}L_{Ni,Ta:Mo})\\ & + {}^2y_{Ni}\,{}^2y_{Ta}({}^1y_{Ni}L_{Ni:Ni,Ta} + {}^1y_{Ta}L_{Ta:Ni,Ta} + {}^1y_{Mo}L_{Mo:Ni,Ta})\\ & + {}^1y_{Ni}\,{}^1y_{Mo}({}^2y_{Ni}L_{Ni,Mo:Ni} + {}^2y_{Ta}L_{Ni,Mo:Ta} + {}^2y_{Mo}L_{Ni,Mo:Mo})\\ & + {}^2y_{Ni}\,{}^2y_{Mo}({}^1y_{Ni}L_{Ni:Ni,Mo} + {}^1y_{Ta}L_{Ta:Ni,Mo} + {}^1y_{Mo}L_{Mo:Ni,Mo})\end{aligned} \quad [3]$$

where ${}^sy_i$ refers to the site fraction of component i in sublattice s. The $^\circ G$ parameter represents the Gibbs energy of a compound in the virtual state of $Ni_3(Mo, Ta)$ and is given relative to the selected reference state for the elements. The symbols in Eqs. [4] through [6] refer to the similar properties. To reduce the number of probable adjustable parameters, the contribution of the interaction between Mo and Ta within the same sublattice was neglected. A same simplification was also introduced into the other intermediate phases.

A four-sublattice model, (Ni, Ta)$_1$(Ta)$_4$(Ni, Ta)$_2$(Ni)$_6$, was used to describe the NiTa phase by Cui and Jin.[7] In the ternary system, only Mo was allowed to substitute for Ta in the second sublattice in order to reduce the number of parameters. A sublattice model with the formula (Ni, Ta)$_1$(Mo, Ta)$_4$(Ni, Ta)$_2$(Ni)$_6$ was thus obtained. The sublattice model yields the following expression for the Gibbs energy for one mole of formula units:

$$\begin{aligned}G_m = {}& {}^1y_{Ni}({}^2y_{Ta}\,{}^3y_{Ni}\,{}^\circ G_{Ni:Ta:Ni:Ni} + {}^2y_{Ta}\,{}^3y_{Ta}\,{}^\circ G_{Ni:Ta:Ta:Ni})\\ & + {}^1y_{Ta}({}^2y_{Ta}\,{}^3y_{Ni}\,{}^\circ G_{Ta:Ta:Ni:Ni} + {}^2y_{Ta}\,{}^3y_{Ta}\,{}^\circ G_{Ta:Ta:Ta:Ni})\\ & + {}^1y_{Ni}({}^2y_{Mo}\,{}^3y_{Ni}\,{}^\circ G_{Ni:Mo:Ni:Ni} + {}^2y_{Mo}\,{}^3y_{Ta}\,{}^\circ G_{Ni:Mo:Ta:Ni})\\ & + {}^1y_{Ta}({}^2y_{Mo}\,{}^3y_{Ni}\,{}^\circ G_{Ta:Mo:Ni:Ni} + {}^2y_{Mo}\,{}^3y_{Ta}\,{}^\circ G_{Ta:Mo:Ta:Ni})\\ & + RT({}^1y_{Ni}\ln {}^1y_{Ni} + {}^1y_{Ta}\ln {}^1y_{Ta}) + 4RT({}^2y_{Mo}\ln {}^2y_{Mo}\\ & + {}^2y_{Ta}\ln {}^2y_{Ta}) + 2RT({}^3y_{Ni}\ln {}^3y_{Ni} + {}^3y_{Ta}\ln {}^3y_{Ta})\\ & + {}^1y_{Ni}\,{}^1y_{Ta}({}^2y_{Ta}\,{}^3y_{Ni}L_{Ni,Ta:Ta:Ni:Ni} + {}^2y_{Ta}\,{}^3y_{Ta}L_{Ni,Ta:Ta:Ta:Ni})\\ & + {}^3y_{Ni}\,{}^3y_{Ta}({}^1y_{Ni}\,{}^2y_{Ta}L_{Ni:Ta:Ni,Ta:Ni} + {}^1y_{Ta}\,{}^2y_{Ta}L_{Ta:Ta:Ni,Ta:Ni})\\ & + {}^1y_{Ni}\,{}^1y_{Ta}({}^2y_{Mo}\,{}^3y_{Ni}L_{Ni,Ta:Mo:Ni:Ni} + {}^2y_{Mo}\,{}^3y_{Ta}L_{Ni,Ta:Mo:Ta:Ni})\\ & + {}^3y_{Ni}\,{}^3y_{Ta}({}^1y_{Ni}\,{}^2y_{Mo}L_{Ni:Mo:Ni,Ta:Ni} + {}^1y_{Ta}\,{}^2y_{Mo}L_{Ta:Mo:Ni,Ta:Ni})\end{aligned} \quad [4]$$

Based on the model of $NiTa_2$ in the binary system,[7] this phase was then described by (Ni, Mo, Ta)$_1$(Mo, Ta)$_2$ in the ternary system. The sublattice model yields the following expression for the Gibbs energy for one mole of formula units:

$$\begin{aligned}G_m = {}& {}^1y_{Ni}({}^2y_{Mo}\,{}^\circ G_{Ni:Mo} + {}^2y_{Ta}\,{}^\circ G_{Ni:Ta})\\ & + {}^1y_{Mo}({}^2y_{Mo}\,{}^\circ G_{Mo:Mo} + {}^2y_{Ta}\,{}^\circ G_{Mo:Ta})\\ & + {}^1y_{Ta}({}^2y_{Mo}\,{}^\circ G_{Ta:Mo} + {}^2y_{Ta}\,{}^\circ G_{Ta:Ta})\\ & + RT({}^1y_{Ni}\ln {}^1y_{Ni} + {}^1y_{Mo}\ln {}^1y_{Mo} + {}^1y_{Ta}\ln {}^1y_{Ta})\\ & + 2RT({}^2y_{Mo}\ln {}^2y_{Mo} + {}^2y_{Ta}\ln {}^2y_{Ta})\\ & + {}^1y_{Ni}\,{}^1y_{Mo}({}^2y_{Mo}L_{Ni,Mo:Mo} + {}^2y_{Ta}L_{Ni,Mo:Ta})\\ & + {}^1y_{Ni}\,{}^1y_{Ta}({}^2y_{Mo}L_{Ni,Ta:Mo} + {}^2y_{Ta}L_{Ni,Ta:Ta})\end{aligned} \quad [5]$$

In the Ni-Mo binary system,[8] the NiMo phase was modeled using a three-sublattice model, (Ni)$_{24}$(Ni, Mo)$_{20}$(Mo)$_{12}$. A ternary model, (Ni)$_{24}$(Ni, Mo, Ta)$_{20}$(Mo, Ta)$_{12}$, was then used, *i.e.*, simply allowing Ta to substitute for Mo. The sublattice model yields the following expression for the Gibbs energy for one mole of formula units:

$$\begin{aligned}G_m = {}& {}^2y_{Ni}({}^3y_{Mo}\,{}^\circ G_{Ni:Ni:Mo} + {}^3y_{Ta}\,{}^\circ G_{Ni:Ni:Ta})\\ & + {}^2y_{Mo}({}^3y_{Mo}\,{}^\circ G_{Ni:Mo:Mo} + {}^3y_{Ta}\,{}^\circ G_{Ni:Mo:Ta})\\ & + {}^2y_{Ta}({}^3y_{Mo}\,{}^\circ G_{Ni:Ta:Mo} + {}^3y_{Ta}\,{}^\circ G_{Ni:Ta:Ta})\\ & + 20RT({}^2y_{Ni}\ln {}^2y_{Ni} + {}^2y_{Mo}\ln {}^2y_{Mo} + {}^2y_{Ta}\ln {}^2y_{Ta})\\ & + 12RT({}^3y_{Mo}\ln {}^3y_{Mo} + {}^3y_{Ta}\ln {}^3y_{Ta})\\ & + {}^3y_{Mo}({}^2y_{Ni}\,{}^2y_{Mo}L_{Ni:Ni,Mo:Mo} + {}^2y_{Ni}\,{}^2y_{Ta}L_{Ni:Ni,Ta:Mo})\\ & + {}^3y_{Ta}({}^2y_{Ni}\,{}^2y_{Mo}L_{Ni:Ni,Mo:Ta} + {}^2y_{Ni}\,{}^2y_{Ta}L_{Ni:Ni,Ta:Ta})\end{aligned} \quad [6]$$

3. *Parameter optimization*

The optimization of parameters was carried out using the Parrot module in the Thermo-Calc program developed by Sundman *et al.*[19] The optimization was performed by several steps. The parameters of fcc, bcc, and liquid phase were first optimized. Then, the parameters of various intermediate phases were optimized one by one. Finally, all the parameters were optimized together to give a better description.

IV. RESULTS AND DISCUSSION

The assessed parameters of each phase are listed in Table IV. Figures 10 through 14 show the comparisons between

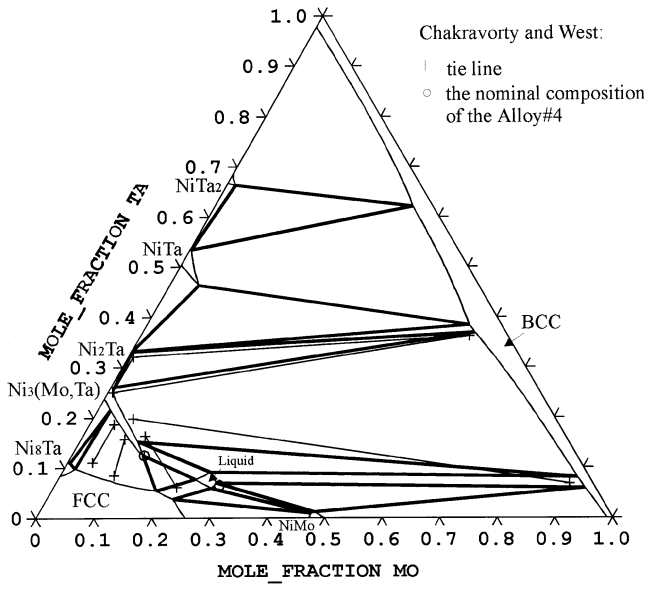

Fig. 10—The calculated isothermal section of the Ni-Mo-Ta system at 1523 K compared with the experimental data.

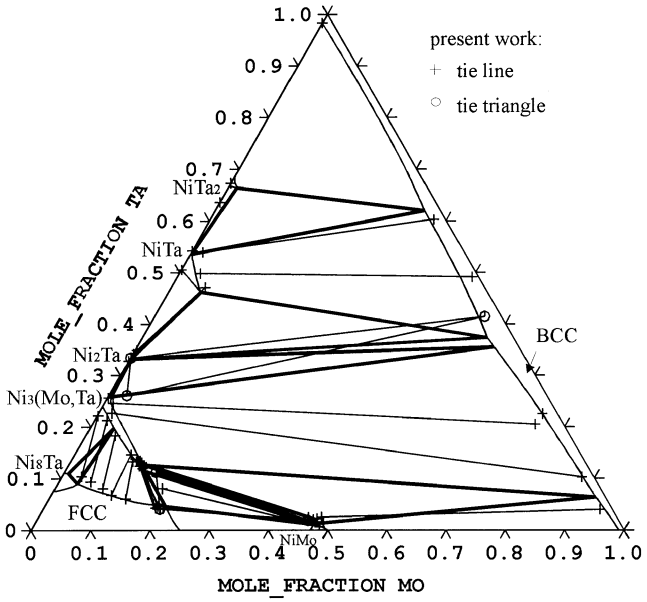

Fig. 11—The calculated isothermal section of the Ni-Mo-Ta system at 1473 K compared with the experimental data.

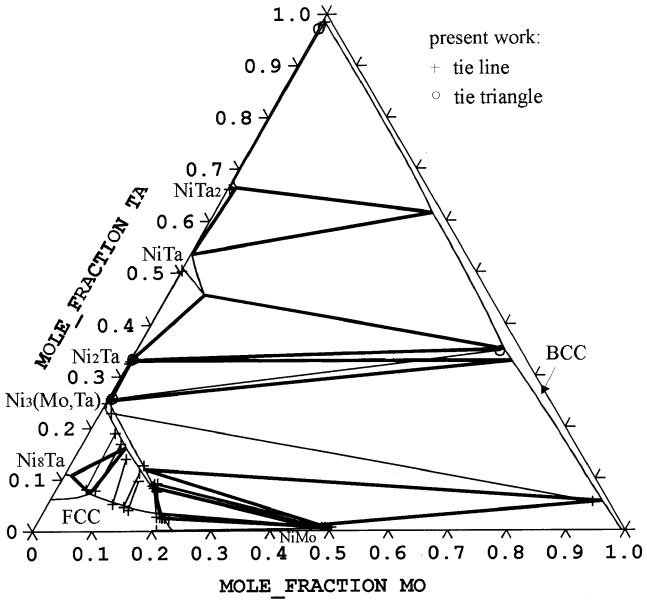

Fig. 12—The calculated isothermal section of the Ni-Mo-Ta system at 1373 K compared with the experimental data.

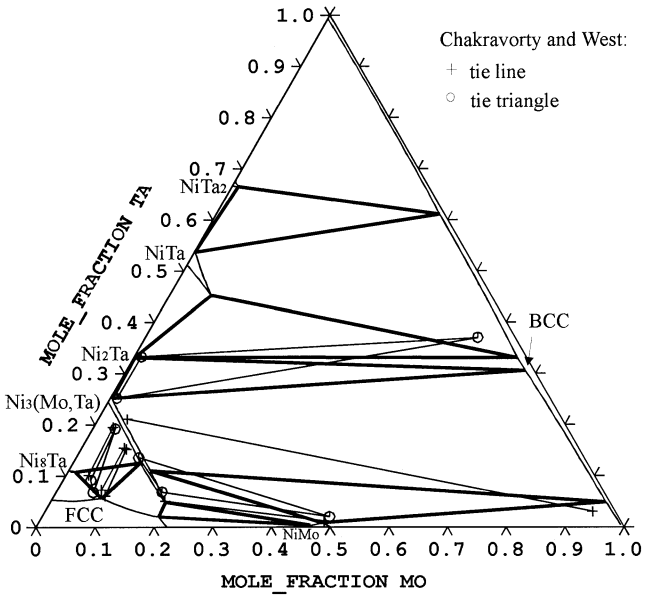

Fig. 13—The calculated isothermal section of the Ni-Mo-Ta system at 1273 K compared with the experimental data.

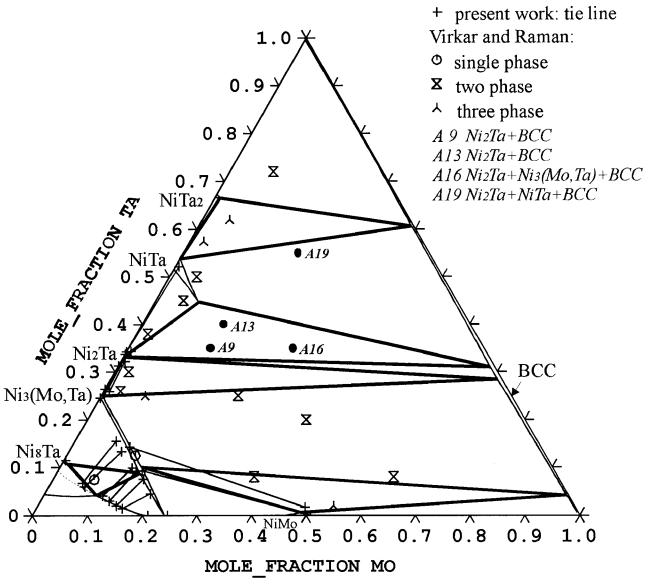

Fig. 14—The calculated isothermal section of the Ni-Mo-Ta system at 1173 K compared with the experimental data.

the calculated isothermal sections and the experimental data at 1523, 1473, 1373, 1273, and 1173 K, respectively. As can be seen from these figures, in most cases, the calculation can reproduce the experimental data within reasonable deviation.

In Figure 10, it can be seen that the liquid phase is stable in the calculated isothermal section at 1523 K. During the assessment, it was found that liquid would be stable even at about 1450 K if no ternary liquid parameters were employed. In view of the experimental isothermal section at 1523 K reported by Chakravorty and West,[2] it is noted that the determined tie-line on alloy 4 (Ni-12.5Mo-12.5Ta, at. pct) did not pass through its nominal alloy composition, unlike any others. Chakravorty and West stated that they could not interpret it. In our views, the reason probably was liquid already formed at this temperature. Considering that the triple at 1473 K in the present experiment has no sign of liquid, the ternary eutectic temperature must lie between 1473 and 1523 K. As a result, a positive value of 30,000 J/mol had to be assigned to the $L_{Ni,Mo,Ta}$ parameter of liquid, though no experimental information of liquid was reported. The value of 30,000 J/mol was obtained by the trial-and-error method.

In Figure 11, the agreement between the calculated and the experimental data at 1473 K is good, with the exception of the tie-triangle $Ni_3(Mo, Ta)/Ni_2Ta/bcc$. However, as indicated in Table I, these data were considered to have great uncertainty and were not used in the assessment.

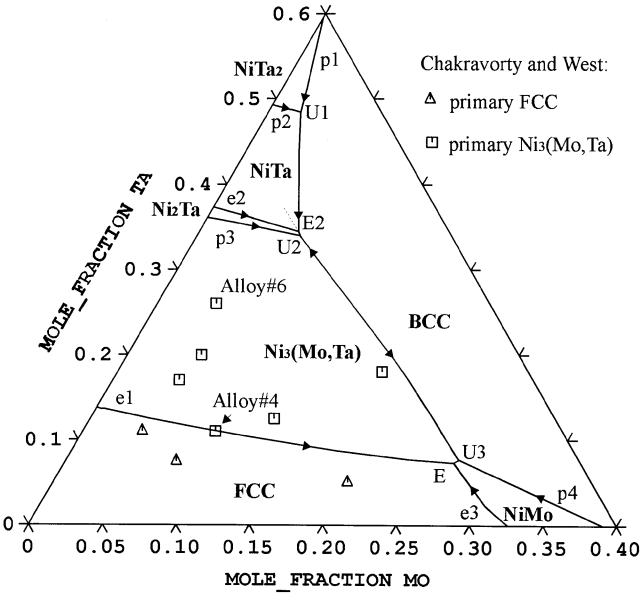

Fig. 15—The calculated liquidus projection of the Ni-Mo-Ta system, along with the experimental points. The dashed line is the metastable monovariant of liq → Ni_2Ta + bcc.

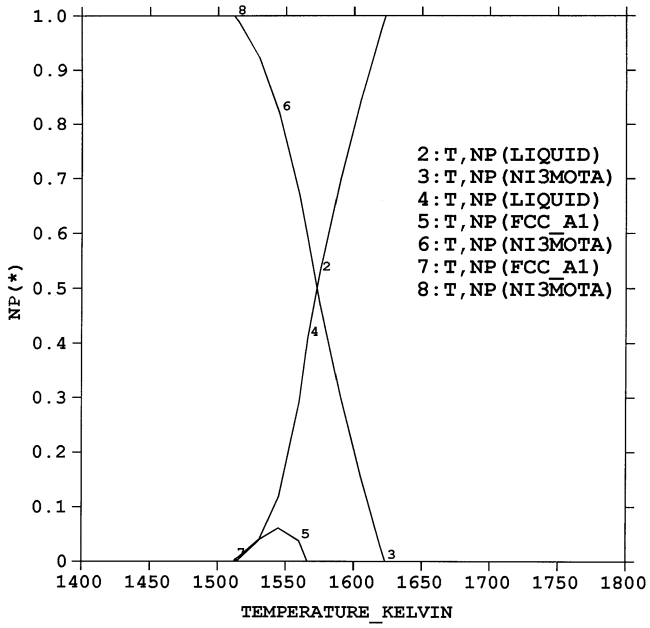

Fig. 16—The calculated numbers of moles of various phase of Ni-12.5Mo-12.5 Ta (at. pct) alloy during the equilibrium solidification.

There is a satisfactory agreement between the calculated phase diagram and the present experimental data at 1373 K, as presented in Figure 12.

As can be seen from Figure 13, there are large discrepancies between the calculation and the experimental data obtained by Chakravorty and West.[2] It is noticed that, however, the alloys used at 1573 K in their study were homogenized for 1 week. Those homogenized alloys were reheated at 1273 K for the same long time to construct the isothermal section at 1273 K. It is also observed that there is no significant difference between the sections at 1273 and 1523 K according to Chakravorty and West.[2] This probably indicates that those alloys at 1273 K had a lack of attainment of equilibrium. Therefore, the section at 1273 K from Chakravorty and West may refer to a section at a higher temperature.

In Figure 14, the calculation fits the present experimental values well. The dashed line is the calculated metastable fcc/Ni_3(Mo, Ta) equilibrium. The experimental data presented by Virkar and Raman[1] are also compared with the calculated phase diagram. In general, the agreement is acceptable with the exception of four alloys containing Ni_2Ta phase, whose constitutions are far from falling within the calculated regions. Those alloys (A9, A13, A16, and A19) are marked in Figure 14.

The calculated liquidus projection of the Ni-Mo-Ta system, along with the experimental points, is presented in Figure 15. The calculation is consistent with the experimental data. The calculation also verifies that a maximum temperature exists in the monovariant reaction of liq ⇔ Ni_3(Mo, Ta) + bcc suggested by Chakravorty and West.[2]

In the following discussions, the present calculation will be applied to explain the solidification behavior of two alloys arc melted by Chakravorty and West.[2] Usually, a simply simulation of solidification behavior can be conducted using the equilibrium model and the Scheil model. The equilibrium model assumes that the equilibrium state is always achieved in the entire solidification procedure, which corresponds to the condition of extremely slow cooling rate; the Scheil model, on the other side, assumes that no back diffusion takes place in solid and perfect mixing occurs in liquid, which applies to an extremely high cooling rate. Such models describe two limit cases.

Chakravorty and West[2] found that the as-cast alloy 4 (75.0Ni-12.5Mo-12.5Ta, at. pct) contained primary crystals of Ni_3(Mo, Ta), fcc, and a small proportion of some regions of the eutectic type. They did not make clear whether the eutectic was a binary mixture of Ni_3(Mo, Ta) + fcc or a ternary mixture containing NiMo also, but reported that its composition was 65.3Ni-28.6Mo-6.1Ta (at. pct). In view of the composition ranges of fcc and Ni_3(Mo, Ta), if no NiMo phases were contained in these eutectic regions, the Ni content of the eutectic could not decrease to 65.3 at. pct, anyway. It was therefore concluded that the eutectic regions observed by Chakravorty and West should be a mixture of the Ni_3(Mo, Ta) + fcc eutectic and the Ni_3(Mo, Ta) + fcc + NiMo ternary eutectic. From Figures 15 and 16, it can be learned that, during the equilibrium solidification of alloy 4, the primary crystals of Ni_3(Mo, Ta) were first formed with the decrease of temperature, then the Ni_3(Mo, Ta) + fcc eutectic was produced. The last drop liquid disappeared before the ternary eutectic reaction temperature *E* was reached. Because this alloy is located so closely to the monovariant of liq ⇔ Ni_3(Mo Ta) + fcc, it was inevitable that some primary fcc form also, as shown in Figure 15. Obviously, this solidification structure conflicts with the experiment by Chakravorty and West. In practice, however, very often the rate of cooling is too rapid to allow substantial diffusion in the solid phase, especially for such a very unlikely equilibrium cooling system. Using the Scheil model, liquid even remained at the temperature of the ternary eutectic reaction *E*, as shown in Figure 17. The ternary eutectic, fcc + Ni_3(Mo, Ta) + NiMo, was subsequently produced from the remaining liquid. Finally, the solidification structure of the alloy would be the primary crystals of Ni_3(Mo, Ta) and fcc, in addition to the

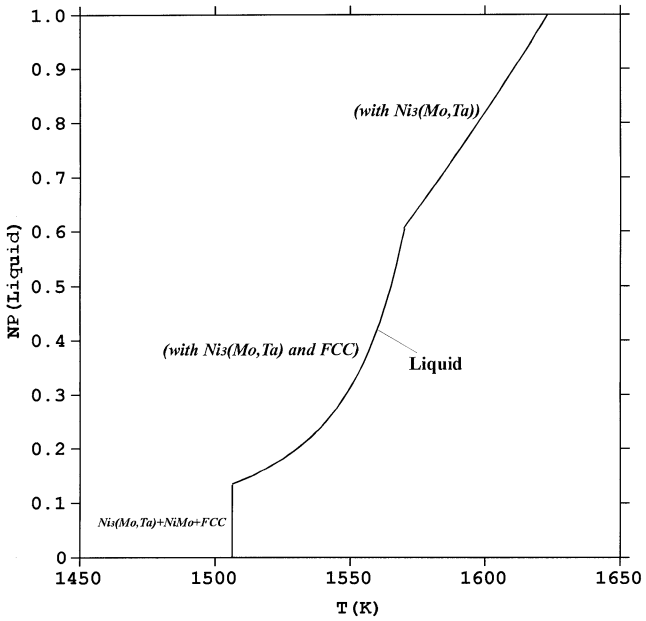

Fig. 17—The calculated number of moles of liquid phase of Ni-12.5Mo-12.5Ta (at. pct) alloy during solidification using the Scheil model.

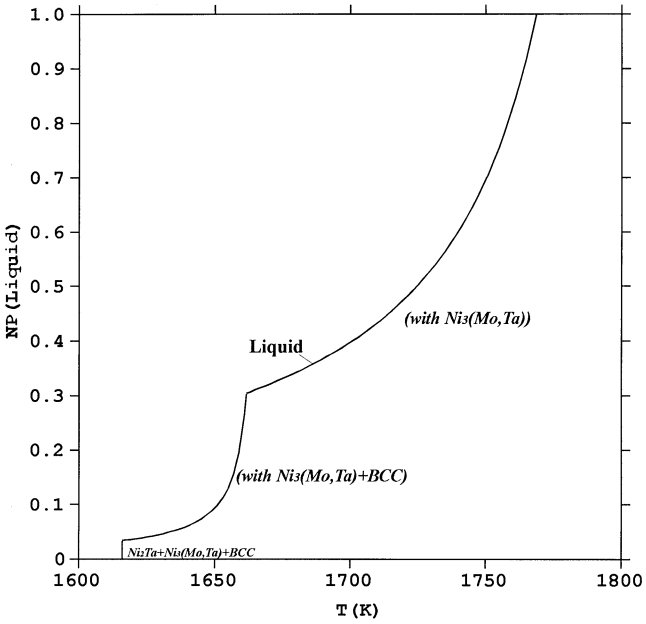

Fig. 18—The calculated number of moles of liquid phase of Ni-4Mo-26Ta (at. pct) alloy during solidification using the Scheil model.

Ni_3(Mo, Ta) + fcc eutectic and the Ni_3(Mo, Ta) + fcc + NiMo ternary eutectic. This structure is in accord with the observation of Chakravorty and West.[2]

Chakravorty and West[2] observed that the as-cast alloy 6 (Ni-4Mo-26Ta, at. pct) contained primary crystals of Ni_3(Mo, Ta), Ni_3(Mo, Ta) + bcc eutectic, and Ni_2Ta + bcc eutectic. Using the Scheil model for alloy 6, the primary crystals of Ni_3(Mo, Ta) were first formed with the decrease of temperature, the Ni_3(Mo, Ta) + bcc eutectic was then produced. Unlike the equilibrium solidification, liquid can even exist at the temperature of the ternary peritectic reaction μ_2, as shown by the calculation in Figure 18. In practice, however, such a ternary peritectic reaction rarely goes to completion. As a result, the remaining liquid would solidify as Ni_2Ta + bcc eutectic along the metastable monovariant of liq $\Leftrightarrow$ Ni_2Ta + bcc (dashed line in Figure 15). Thus, the final structure of the as-cast alloy would be the primary crystals of Ni_3(Mo, Ta), along with the Ni_3(Mo, Ta) + bcc and Ni_2Ta + bcc eutectics. This structure was confirmed by the observation of Chakravorty and West.[2]

V. CONCLUSIONS

1. The phase equilibrium data of the Ni-Mo-Ta system at 1473, 1373, and 1173 K were determined by means of diffusion couple and EPMA technique.
2. The Ni-Mo binary system was successfully modified based on the assessment of Frisk,[8] and a better thermodynamic description of each phase was given.
3. The Mo-Ta binary system was assessed and a set of thermodynamic descriptions was obtained.
4. The Ni-Mo-Ta ternary system was assessed, and a consistent thermodynamic description of the Ni-Mo-Ta system was obtained. A number of calculated isothermal sections were presented and compared with the experimental data. The calculation, in most cases, can reproduce the experimental data within reasonable deviation. The present calculation has been successfully used to analyze the solidification behavior of some alloys.

ACKNOWLEDGMENTS

This work was financially supported by GE Company, under Research Contract No. 9622031. The authors are grateful to Dr. J.C. Zhao (R&D, GE Company) for his valuable advice regarding this work. We thank Mrs. Xiulin Han (The Geology Institute, Chinese Academy of Science) for her help with the EPMA. We also thank Mr. Z.Y. Liu for his helpful comments on the manuscript.

REFERENCES

1. A.V. Virkar and A. Raman: *Z. Metallkd.*, 1969, vol. 60, pp. 594-600.
2. S. Chakravorty and D.R.F. West: *Met. Sci.*, 1983, vol. 17, pp. 573-80.
3. K.P. Gupta: *J. Alloy Phase Diagrams*, 1990, vol. 6, pp. 86-95.
4. L. Kaufman: *CALPHAD*, 1991, vol. 15, pp. 261-82.
5. L. Kaufman: *CALPHAD*, 1991, vol. 15, 243-59.
6. I. Ansara and M. Selleby: *CALPHAD*, 1994, vol. 18, pp. 99-107.
7. Y. Cui and Z. Jin: *Z. Metallkd.*, 1999, vol. 90, pp. 233-41.
8. K. Frisk: *CALPHAD*, 1990, vol. 14, pp. 311-20.
9. R.E.W. Casselton and W. Hume-Rothery: *J. Less-Common Met.*, 1964, vol. 7, pp. 212-21.
10. C.P. Heijwegen and G.D. Rieck: *Z. Metallkd.*, 1973, vol. 64, pp. 450-53.
11. P.J. Spencer and F.H. Putland: *J. Chem. Thermodyn.*, 1975, vol. 7, pp. 531-36.
12. O. Kubaschewski and T. Hoster: *Z. Metallkd.*, 1983, vol. 74, p. 607.
13. H. Buckle: *Metallforsch.*, 1946, pp. 53-56.
14. G.A. Geach and D.S. Smith: *J. Inst. Met.*, 1951, vol. 80, pp. 143-47.
15. E. Rudy: Report. No. AFML-tr-65-2, Part V, Air Force Materials Laboratory, Wright Patterson AFB, OH, 1969.
16. T.B. Massalski, J.L. Murray, L.H. Bennett, and H. Baker: *Binary Alloy Phase Diagrams*, ASM, Metals Park, OH, 1986, pp. 1634-45.
17. S.C. Singhal and W.L. Worrel: *Metallurgical Chemistry*, Proc. Symp., 1971, O. Kubaschewski, ed., Her Majesty's Stationary Office, London, 1972, pp 65-74.
18. A. Dinsdale: *CALPHAD*, 1991, vol. 15, pp. 317-425.
19. B. Sundman, B. Jansson, and J. O. Andersson: *CALPHAD*, 1985, vol. 9, pp. 153-90.